Available online at www.sciencedirect.com
ScienceDirect
Journal of Electroanalytical Chemistry 602 (2007) 203–209
Journal of Electroanalytical Chemistry
www.elsevier.com/locate/jelechem

In situ conductance and *in situ* ATR-FTIR study of poly(*N*-methylaniline) in aqueous solution

Di Wei [a,b], Pamela Espindola [c], Tom Lindfors [a], Carita Kvarnström [a,*], Jürgen Heinze [c], Ari Ivaska [a]

[a] *Process Chemistry Centre, c/o Laboratory of Analytical Chemistry, Åbo Akademi University, Biskopsgatan 8, 20500 Åbo/Turku, Finland*
[b] *Graduate School of Materials Research (GSMR), Åbo Akademi University, 20500 Åbo/Turku, Finland*
[c] *Institut für Physikalische Chemie, FMF, Universität Freiburg, Albertstr. 21a, D-79104 Freiburg i. Br, Germany*

Received 19 July 2006; received in revised form 14 December 2006; accepted 20 December 2006
Available online 12 January 2007

Abstract

In situ attenuated total reflection Fourier transform infrared spectroscopy, ATR-FTIR and *in situ* conductance measurements offer information on structure, electronic, and conductance changes during doping and electropolymerization of conducting polymers. In this paper, we report the *in situ* recording of the conductance changes during cyclic voltammetry measurements (electropolymerization and the subsequent doping) of *N*-methylaniline (NMA). The vibrational spectra of poly(*N*-methylaniline) (PNMA) show specific and characteristic features not only related to its chemical structure, but also to the existence of free charge carriers delocalized along the π-electron network. Results from both *in situ* conductance and *in situ* ATR-FTIR have brought us a better understanding of electronic properties and the nature of charge carriers of PNMA film synthesized in acidic aqueous solutions.

Keywords: Poly(*N*-methylaniline); Electropolymerization; *In situ* ATR-FTIR; *In situ* conductance

1. Introduction

Conductance is an essential parameter when constructing polyaniline-based microelectronic devices as diodes and transistors [1–3]. New organic electronics can be designed by functionalizing polyaniline (PANI) at the nitrogen atom. *N*-grafting of PANI is also expected to affect the electrical conductivity. Recently, Yasuda et al. prepared *N*-substituted PANI with oligo-ether side chains using ring-opening graft copolymerization of epoxide [4]. The resulting copolymers showed both electrochemical and electrochromic activity during redox switching.

The mechanism of charge transport in conducting polymers has been intensively studied since the report of an insulator to metal transition in polyacetylene [5]. Many non-degenerate ground state polymers such as polythiophene (PT) and polypyrrole (PPy) have also been studied in this aspect [6,7]. PANI is different from these well known conducting polymers in the following important aspects. First, the Fermi level and the band gap of PANI are not formed in the center of the band, resulting in asymmetric valence and conduction bands. A single broad polaron band appears deep in the gap instead of two, and another very narrow band appears near the conduction-band edge in PANI [8]. Second, in contrast to PPy, which nitrogen atoms do not contribute significantly to the conjugation [9], both carbon rings and nitrogen atoms are within the conjugation path in PANI. Third, the electronic state of PANI can be altered through variation of either the number of electrons or the number of protons. Monkman et al. [10] concluded that the conduction mechanism in PANI is mainly inter and intra chain hopping between localized charge sites on the polymer backbone. One big difference between PNMA and PANI is that PNMA is

* Corresponding author. Tel.: +358 2 215 4419; fax: +358 2 215 4479.
E-mail addresses: carita.kvarnstrom@abo.fi, ckvarnst@abo.fi (C. Kvarnström).

0022-0728/$ - see front matter © 2007 Elsevier B.V. All rights reserved.
doi:10.1016/j.jelechem.2006.12.017

not that pH sensitive [11], which means only the oxidation levels (applied potentials) alter the conductance in the acidic media used.

One of the main tasks concerning conductivity of conducting polymers has been to determine the nature of the charge carriers responsible for the electronic conduction in these materials. The conduction mechanism of PNMA was explained by Lian et al. as variable-range hopping (VRH) of the charge carriers. Their results were obtained from studies of the broadband dielectric and conducting properties of different poly(*N*-alkylanilines) [12]. The conductivity was measured to 5.7×10^{-2} S m^{-1} of the emeraldine form of PNMA, in comparison to the value of 10^{-7} S m^{-1} obtained for the same polymer in its non-conducting form. The dependence of the length of the *N*-substituted chain on the conductivity of the PANI derivatives was studied by Yano et al. by measuring pellets made from the polymers with the four probe technique [13]. Kankare et al. [14] proposed a theoretical model for the conductance of a growing conducting polymer layer on a double-band electrode. The instrument design of various types of *in situ* conductivity measurements and their application on electrochemically synthesized conducting polymers, have been demonstrated in some publications [15–18]. However, there are only a few reports on the conductivity studies of PNMA [12,13,19,20]. *In situ* conductance measurements on PNMA carried out simultaneously with voltammetric measurements in an electrochemical cell have to the best knowledge of the authors, not earlier been reported.

In situ ATR-FTIR was used to study the spectroelectrochemical behavior of PNMA films upon electrochemical p-doping. The doping induced infrared active vibration (IRAV) bands, which rise in the infrared spectrum due to charging, are caused by a strong electron–phonon coupling in the conjugated polymers. The intensity of the IRAV bands increases successively with increasing doping level. New energy states will be created upon doping of conjugated polymers within the gap between the valence band and the conduction band. Thus, at higher energy (wavenumbers) electronic absorption bands appear, which are correlated to transitions of newly created states of charged quasi-particles, usually described as polarons in the band gap [21]. In all the attempts to explain the origin of the IRAV pattern, there is a strong link between the effective conjugation of the conducting polymer, effective delocalization of the doping induced quasi-particle excitations, and the signatures of the IRAV bands in the doping induced infrared spectrum [21]. Therefore, the correlation between conductance, the electronic absorbance and the IRAV bands will offer a better understanding of the electronic properties in the polymer.

In this work, both *in situ* conductance and *in situ* ATR-FTIR measurements were performed on PNMA in an aqueous solution containing 1.0 M trifluoroacetic acid (CF_3COOH). Using CF_3COO^- as counter ion in electrochemical doping is beneficial for IR spectroscopic measurements because the absorption bands originating from the anions are well separated from the absorption bands of PANI [22]. We consider the same is valid for PNMA.

2. Experimental

2.1. Chemicals

N-methylaniline (NMA) (98.0%), was obtained from Fluka and trifluoroacetic acid (CF_3COOH) (99%) from Aldrich. All chemicals were used as received. Solutions were prepared from the deionized water purified through a Maxima ultrapure water system (ELGA, 18.2 MΩ cm). All solutions were purged with nitrogen prior to use.

2.2. In situ conductance

The microarray working electrode (WE), which consists of two closely spaced platinum (Pt) electrodes of comb shape, was used for *in situ* conductance measurements of electrochemically synthesized PNMA. The microarray WE with a gap distance of 5 μm was separated from the potentiostat by two 1 kΩ resistors. A bias of 10 mV was applied to the microarray and the potential was measured at a third 1 kΩ resistor. The conductance (*S*) can only be measured when the conducting polymer covers the gaps between the strips of the comb electrodes. Since the current which flows additionally from one part of the comb to the other part can be measured, the conductance of the PNMA film on the microarray electrode was obtained using Ohm's law. The PNMA film was deposited on the two-band electrode, which was introduced by Heinze et al. [23,24] and the conductance was monitored simultaneously during cyclic voltammetry measurements. The polymerization was carried out in aqueous solution containing 0.5 M NMA and 1.0 M CF_3COOH in a three-electrode cell. Ag/AgCl (Ag wire coated with AgCl) was used as reference electrode (RE), and a Pt wire as the counter electrode (CE). The polymerization potential range was set between −0.3 V and 0.6 V, and 40 cycles were made, at a scan rate of 20 mV/s. *In situ* conductance was also recorded during the subsequent doping of the PNMA film. The doping was done in a monomer-free aqueous solution containing 1.0 M CF_3COOH, in the potential range of −0.3 V to 0.3 V or 0.5 V (20 mV/s, 4 cycles). Since the area and the film thickness were not known precisely, we did not convert the conductance data into specific conductivities in this work.

2.3. In situ ATR-FTIR

The spectroelectrochemical behavior of PNMA films and the doping induced IRAV absorption bands arising upon electrochemical p-doping were investigated by *in situ* ATR-FTIR measurements, where a Bruker IFS66/S spectrometer with an MCT detector was used. The spectra were measured with a spectral resolution of 4 cm^{-1}. The

details of the set up have been described earlier [21]. A ZnSe reflection element, sputtered with a thin layer of Pt, was used as the WE and as a waveguide for the IR radiation. Information about the structure of the PNMA film deposited at the WE can be obtained due to the attenuated reflectance of the ZnSe element of the IR radiation in the ATR spectroscopy.

The PNMA film was electropolymerized in the same way as in the conductance measurement from an aqueous solution containing 0.5 M NMA and 1.0 M CF_3COOH. The potential was controlled by an Autolab (PGSTAT 20) potentiostat within an interval of −0.3 V to 0.6 V. The polymerization was made by 40 cycles with a scan rate of 20 mV/s. A Pt foil was used as CE and Ag/AgCl as the RE. After the polymerization, spectral changes of the PNMA film were recorded simultaneously as the potential was slowly scanned (5 mV/s) between −0.3 V and 0.5 V in 1.0 M CF_3COOH aqueous solution for 1–2 cycles. To distinguish between the characteristic spectral changes from the specific electrochemical reaction process studied and changes induced by the instrument or the electrolyte, a reference spectrum is chosen just before the potential where the considered reaction takes place. In our case, a reference spectrum was measured at −140 mV, where the PNMA film was in its fully reduced leucoemeraldine form (LE). The other spectra were related to this reference during p-doping, and each spectrum covers the range of approx. 80 mV in the cyclic voltammogram.

3. Results and discussion

3.1. In situ conductance

The conductance of the PNMA film was first recorded during the polymer formation by cyclic voltammetry in the potential range between −0.3 V and 0.6 V. As the polymerization proceeds, the conductance increases due to the deposition of polymeric materials on the electrode.

Fig. 1 shows that the conductance is higher in the reverse scan (reduction) than in the forward scan (oxidation) during the electropolymerization. Earlier results reported on the potentiodynamic electrosynthesis of PPy and polybithiophene, showed that the formed oligomers were soluble during oxidation, while during discharging they were immediately deposited at the electrode [25]. The studied oxidized oligomers have as stated by Heinze et al. [25] a higher solubility than the neutral species.

Previous investigations in the group of Heinze [26] using a quartz micro balance showed that the decrease of mass during discharging start at very positive potentials. This is caused when ions and solution molecules were leaving the film matrix during the cathodic sweep. The structure is getting more compact and the electron hopping is improved. As a result we get higher conductance values during the discharging of the film.

The reason for the lower conductance in the consecutive forward scan in comparison to the previous reverse scan

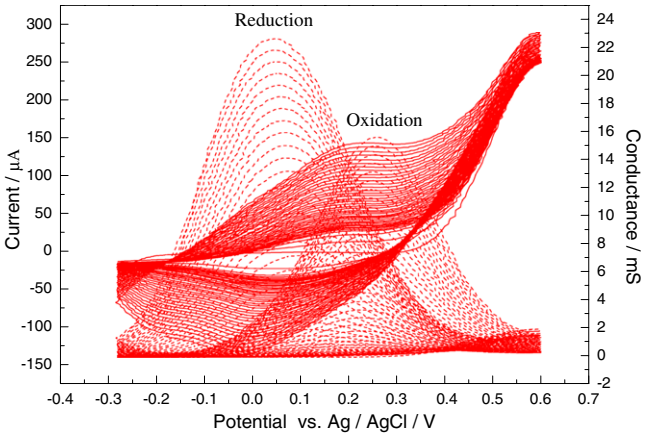

Fig. 1. *In situ* conductance measurement recorded during electropolymerization of 0.5 M NMA in water containing 1.0 M CF_3COOH. The conductance changes, dashed line (---), were recorded during cyclic voltammetry: −300 mV to 600 mV, 20 mV/s, and 40 cycles. Solid line shows the CV response.

can be from the difference in charge distribution in the film. The charge distribution is time dependent and may not reach an optimum during the forward scan. The difference in conductance between charging and discharging of the film has been observed in other conducting polymers as well [27]. It should also be noted that, the synthesis and doping occurs simultaneously with electrochemical techniques. Therefore, it may be difficult to separate the contributions originating from the doping and the polymerization especially in the latter cycles of the polymerization.

In Fig. 2, the conductance is shown as a function of potential during electrochemical doping of a PNMA film in aqueous solution containing 1.0 M CF_3COOH. PNMA is considered to exist in three redox states [28], i.e. the fully reduced leucoemeraldine (LE) form, the only conducting emeraldine (E) form and the fully oxidized pernigraniline (PN) form. The structures of the different forms of PNMA are drawn in Scheme 1 [29,30].

The LE and the PN will be the predominant forms at the potential range below −0.2 V and above 0.5 V, respectively. The peak potentials of the reversible conversion of the LE/E forms can be observed at $E_{p1,ox} = -15$ mV and $E_{p1,red} = -218$ mV. Thus, the LE to E transition takes place approximately at the average potential, $E_{p1,1/2} = -117$ mV. The middle pair of peaks in the cyclic voltammogram is attributed to the degradation and formation of by-products [31]. Since the redox peaks from the reversible E/PN transition appear at $E_{p2,ox} = 422$ mV and $E_{p1,red} = 321$ mV, the E to PN transition potential ($E_{p2,1/2}$) is approximately 371 mV. At a potential range between −117 mV and 371 mV, the E form will dominate, which will cause a big increase in conductance. Based on the theory of a hopping process reported for charge carriers in different conducting polymers, it is stated that the number of free places for charge carriers on the polymer chain decreases with increasing charging level for systems with short conjugation length, which is the case for electrosynthesized conjugated

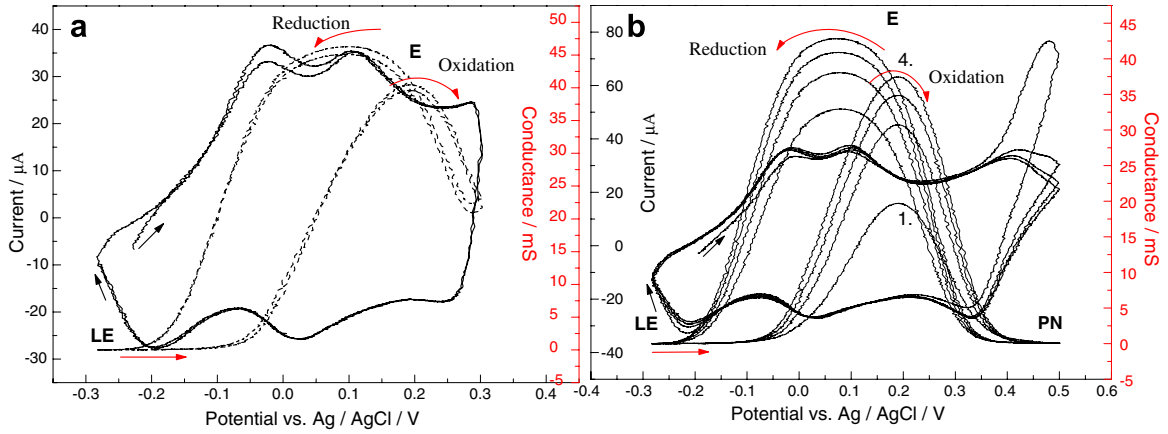

Fig. 2. *In situ* conductance measurement recorded during doping of the PNMA film, which was performed by cyclic voltammetry in 1.0 M CF_3COOH aqueous solution at a scan rate of 10 mV/s, −300 mV to 300 mV, and 4 cycles (a) and at a scan rate of 10 mV/s, −300 mV to 500 mV, and 4 cycles, the first and last scans are indicated (b).

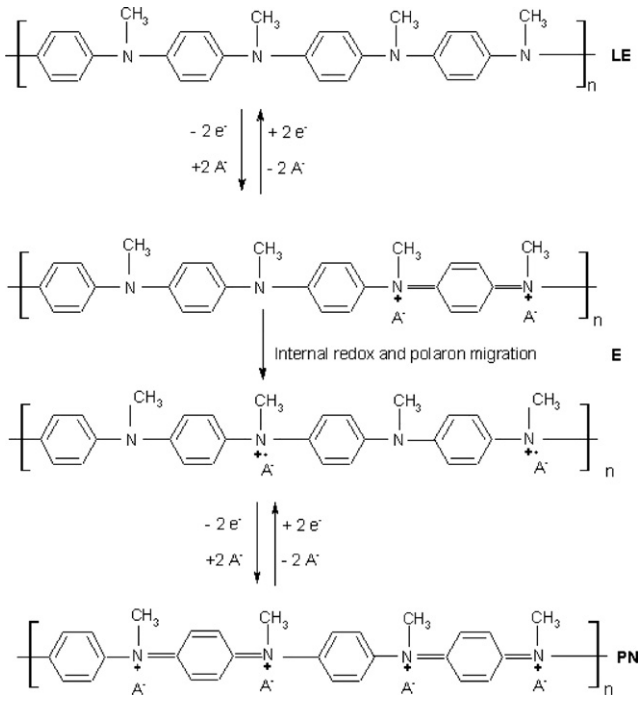

Scheme 1. The structure of the different forms of PNMA, leucoemeraldine (LE), emeraldine (E) and pernigraniline (PN).

polymers. When the potential is high enough, all energetically equivalent sites are occupied and the conductance decreases.

The highest conductance value during p-doping appears at approximately 190 mV. Similarly as in the polymerization, the conductance is higher during the reductive cycles than during the oxidation cycles. It should be noted that the voltammetric measurements have been carried out in a strongly acidic solution. Consequently, a protonated LE form of the polymeric system has been oxidized during the voltammetric scan which induces a positive shift of the oxidation potential. After oxidation the polymer will be partly deprotonated leading to the highly conducting emeraldine form. During the reverse scan the conductivity increases again. Its highest value lies at more negative potential than that of the oxidation scan. A reason for this shift may be that the P/E transition occurs at a lower potential due to the fact that a deprotonated species will be reduced first. In Fig. 2a, the potential cycling is made within a potential range (−0.3 V to 0.3 V) where neither the transition of E/PN nor the degradation takes place. A slight decrease in conductance at high potentials is observed mainly due to charge carrier localization. The conductance curve is reproducible upon consecutive cycling of the film. In Fig. 2b, the potential range is extended to 0.5 V. In the end of the scan the PN form of PNMA is dominating, and the conductance is decreasing, because all energetically equivalent sites are occupied. The measured conductance is growing with every potential cycle. As explained before, this may be due to the time-dependent charge distribution and the polymer backbone rearrangement. During the conversion of E to PN, it is well known that some degradation processes also take place [32]. Degradation leads to a by-product formation. The presence of these species can be seen as a third peak in the voltammogram in between the redox peaks from the LE/E and E/PN transitions of PNMA. The part of the film that undergoes this degradation looses its conjugation, but is still redox active giving rise to faradaic currents. In the conductance measurements, the current between the comb electrodes is measured, and the measured current keeps growing with increasing number of doping cycles (−0.3 V to 0.5 V) due to the progressive formation of redox active degradation products formed during consecutive cycling. In order to further study the effective conjugation length during doping, *in situ* ATR-FTIR measurements were performed.

3.2. In situ ATR-FTIR

The doping response of the PNMA film deposited on the ZnSe reflection element with a sputtered Pt surface is

shown in Fig. 3 (inset). The results of the *in situ* ATR-FTIR measurements (8000–500 cm^{-1}) from p-doping of PNMA are displayed in Fig. 3. The spectra measured at different potentials have been separated from each other and in order to clarify the changes only chosen spectra are displayed. An enlargement of the IRAV region (1700–650 cm^{-1}) is shown in Fig. 4.

Upon charging, a broad electronic absorption maximum at approx. 6500 cm^{-1}, associated with the presence of free charge carriers [33] is growing until the applied potential exceeds 180 mV as shown in Fig. 3. At higher applied potentials the intensity of the electronic absorption band decreases indicating that the free charge carriers are gradually localized. The absorption maximum centred at around 7710 cm^{-1} appears when the applied potential exceeds 340 mV. The shift of the maximum to higher energy is due to the transition from the conducting E form to the non-conducting PN form of PNMA. This is in good agreement with the transition potential ($E_{p2,1/2}$) estimated from Fig. 2, which is approximately 371 mV. The absorbance bands become negative after 420 mV, this may be due to the thickness and electrochromic properties of the PNMA film, which itself influences the reflectance from the film in the ATR geometry.

Simultaneously as the electronic absorbance starts to develop, the vibrational spectra of the PNMA film, in the region below 2000 cm^{-1}, show strong effects during the doping process. This is due to strong electron–phonon coupling within the polymer backbone. Doping induced IRAV bands grow in intensity with the degree of oxidation of the PNMA film. As discussed above, there are two different electrochemical doping processes for PNMA in acidic aqueous solutions. The first occurs via conversion of the

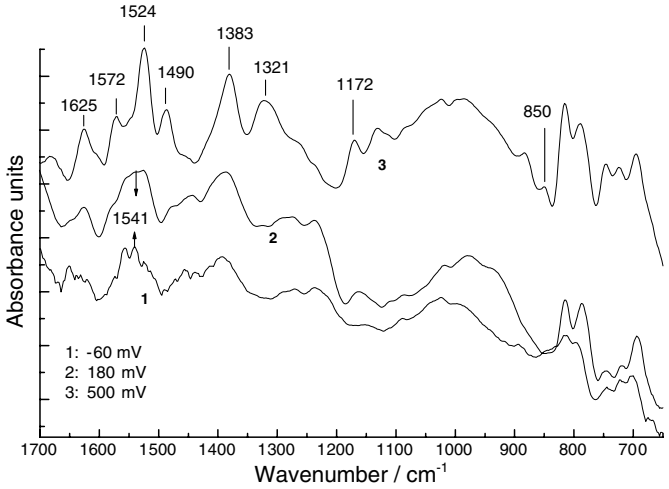

Fig. 4. Enlargement of the IRAV region for the *in situ* ATR-FTIR spectra of PNMA film with wavenumbers 1700–650 cm^{-1}.

LE form into the conducting E form. In this process, some of the benzenoid structures change into quiniod structures. The characteristics of the IR bands between 1450 cm^{-1} and 1700 cm^{-1} in Fig. 4 indicates an aromatic ring transformation from a benzenoid to a more quinoid structure [34]. The absorption intensities at 1321 cm^{-1}, 1383 cm^{-1}, 1490 cm^{-1}, and 1625 cm^{-1} appear to be more pronounced when the potential was increased to 180 mV. At higher potentials, the bands still increase in intensity and become sharper. The band at 1321 cm^{-1} is characteristic of the C–N stretching and C–H bending vibrational transitions. A direct transformation of aromatic rings giving rise to the band at 1541 cm^{-1}, into an alternating benzenoid–quinoid ring sequence, typical for the E form of PNMA can be

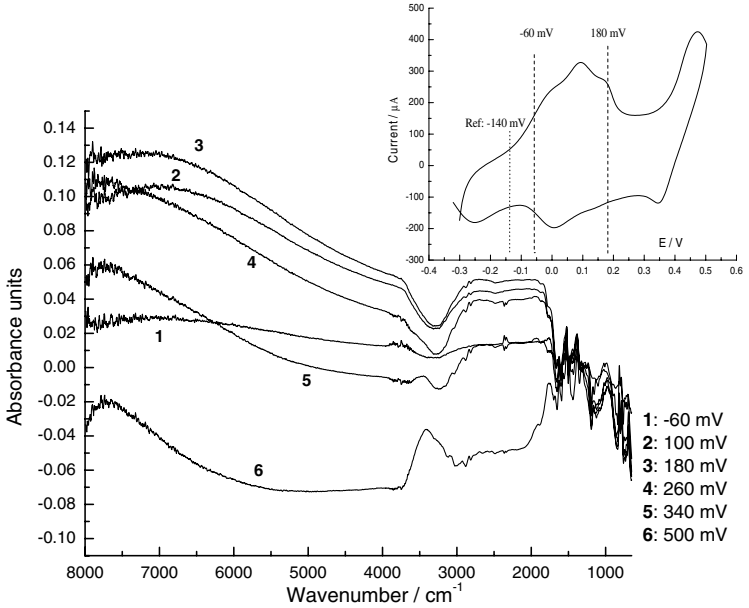

Fig. 3. *In situ* ATR-FTIR spectra of the PNMA film in 1.0 M CF_3COOH aqueous solution during p-doping by anodic potential sweep from −300 mV to 500 mV. The scan rate was 5 mV/s and the reference spectrum was taken at −140 mV. Inset: cyclic voltammogram of the PNMA film in 1.0 M CF_3COOH aqueous solution: −300 mV to 500 mV, 5 mV/s, 1 cycle.

observed. Bands at 1572 cm^{-1} (ring stretching), 1625 cm^{-1} (N=ring vibrations) and 1172 cm^{-1} (C–H in plane bending vibration) indicate the formation of a para-substituted semiquinoid form [19,35]. The E to PN transition is characterized by the further creation of quinoid structures with bands at 1172 cm^{-1}, 1572 cm^{-1}, 1625 cm^{-1} and the C–H out of plane bending vibration at 850 cm^{-1}. When the applied potential exceeds 180 mV, all these bands become continuously more pronounced, which indicate that more quinoid structures are formed in the PNMA backbone.

After the reduction scan, the PNMA film reaches again its original neutral state. On subsequent p-doping with an extended potential window (−0.3 V to 0.6 V), similar behaviour can again be observed. The free charge carrier absorbance band at 6500 cm^{-1} starts to decrease when the applied potential exceeds 192 mV. This is in good accordance with the potential value (190 mV) where the highest p-doping currents are obtained in the *in situ* conductance measurements as shown in Fig. 2. Monkman et al. [10] observed the first clear evidence of semiquinone (polaron) formation at an oxidation potential of ca. 200 mV vs. Ag/AgCl. Our critical potential at ca. 190 mV matches this polaron formation potential.

4. Conclusions

In the field of conjugated polymers, doping means charge transfer, no matter it is by oxidation (p-type doping) or reduction (n-type doping). Doping induces modifications in both the chemical structure and the electronic properties of the polymer. The doped polymers show increased electrical conductance due to doping induced charge carriers in the polymer chain.

PNMA is a non-degenerate conducting polymer. Generally speaking, two possibilities of the charge carriers, polarons and bipolarons, may exist in non-degenerate conducting polymers like PNMA. Debates whether the optical spectrum for the conducting form of PANI/PNMA results from the presence of bipolarons or a polaron lattice has been going on. Later, it was found later that it largely depends on different methods of preparation [36].

The sole optical spectroscopic measurement cannot clearly distinguish polarons and bipolarons, since both charge carriers generate quinoid structures. However, it may provide a new way to figure out the most possible charge carrier created for PANI type material when combining *in situ* ATR-FTIR with the conductance measurements. In the higher energy region of *in situ* ATR-FTIR spectroscopy, the information on conductance can be acquired. It offers the opportunity to observe the induced charge carriers by doping. In the lower energy region, IRAV bands will give us structure information of the formed PNMA film. Both *in situ* conductance and *in situ* ATR-FTIR measurements show that the potential where most free charge carriers were created during p-doping is at ca. 190 mV. At this potential the generation of semiquinones (polarons) was reported [10]. Specific absorption bands like 1172 cm^{-1} were observed at this potential in the ATR-FTIR spectrum that can be considered as evidence for formation of semiquinoidic structures. At higher potentials, more quinone structure will be generated, and the charge carrier will become localized, thus the conductance goes down. High conductance occurs only when the conjugated polymer contains both charged and uncharged sites, so that the charge species can hop along the polymer backbone.

For electrochemical doping of PNMA film in solutions, two different processes should exist. The first oxidation process converts LE form to E form resulting in the highly conductive polaron lattice state. It is accompanied by the generation of free charge carrier absorption ~6500 cm^{-1}. The second oxidation process converts the E form into PN form, and the free charge carrier absorption vanishes simultaneously. The development of degradation products during the conversion of the material to the PN form influences the effective conjugated length and may interfere the *in situ* conductance measurement due to their own redox response giving rise to Faradaic currents as shown in Fig. 2b. Our study showed that the conducting E form of PNMA will dominate in the potential region between around −117 mV to 371 mV in 1 M CF_3COOH aqueous solution.

Acknowledgement

This work is part of the activities of the Åbo Akademi Process Chemistry Centre within the Finnish Centre of Excellence Programme (2000–2011) supported by the Academy of Finland.

References

[1] E.T.T. Jones, O.M. Chyan, M.S. Wrighton, J. Am. Chem. Soc. 109 (1987) 5526.
[2] E.P. Lofton, J.W. Thackeray, M.S. Wrighton, J. Phys. Chem. 90 (1986) 6080.
[3] E.W. Paul, A.J. Ricco, M.S. Wrighton, J. Phys. Chem. 89 (1985) 1441.
[4] T. Yasuda, I. Yamaguchi, T. Yamamoto, J. Mat. Chem. 13 (2003) 2138.
[5] H. Shirakawa, E.J. Louis, A.G. MacDiarmid, C.K. Chiang, A.J. Heeger, J. Chem. Soc. Chem. Commun. (1977) 578.
[6] R. Qian, J. Qiu, D. Shen, Synth. Met. 18 (1987) 13.
[7] C. Taliani, R. Danieli, R. Zamboni, P. Ostoja, P. Porzio, Synth. Met. 18 (1987) 177.
[8] S. Stafström, J.L. Bredas, A.J. Epstein, H.S. Woo, D.B. Tanner, W.S. Huang, A.G. MacDiarmid, Phys. Rev. Lett. 59 (1987) 1464.
[9] J.L. Bredas, B. Themans, J.M. Andre, Phys. Rev. B 27 (1983) 7827.
[10] A.P. Monkman, D. Bloor, G.C. Stevens, J.C.H. Stevens, P. Wilson, Synth. Met. 29 (1989) 277.
[11] T. Lindfors, A. Ivaska, J. Electroanal. Chem. 38 (2002) 1791.
[12] A. Lian, S. Besner, L.H. Dao, Synth. Met. 74 (1995) 21.
[13] J. Yano, Y. Ota, A. Kitani, Mater. Lett. 58 (2004) 1934.
[14] J. Kankare, E.L. Kupila, J. Electroanal. Chem. 322 (1992) 167.
[15] L.O.I. Chanteloube, A. Germain, M. Petit, E.M. Genies, Synth. Met. 30 (1989) 159.
[16] R. Holze, J. Lippe, Synth. Met. 38 (1990) 99.
[17] M.C. Morvant, J.R. Reynolds, Synth. Met. 92 (1998) 57.
[18] M. Probst, R. Holze, Electrochim. Acta 40 (1995) 213.

[19] S.K. Manohar, A.G. MacDiarmid, K.R. Cromack, J.M. Ginder, A.J. Epstein, Synth. Met. 29 (1989) 349–356.
[20] J.J. Langer, Synth. Met. 35 (1990) 295.
[21] C. Kvarnström, A. Ivaska, H. Neugebauer, in: H.S. Nalwa (Ed.), Advanced Functional Molecules and Polymers, vol. 2, Gordon & Breach Science Publishers, 2001 (chapter 6).
[22] Z. Ping, H. Neugebauer, A. Neckel, Electrochim. Acta 41 (1996) 767.
[23] M. Pagels, J. Heinze, B. Geschke, V. Rang, Electrochim. Acta 46 (2001) 3943.
[24] M. Zhou, M. Pagels, B. Geschke, J. Heinze, J. Phys. Chem. B 106 (2002) 10065.
[25] J. Heinze, R. Bilger, C. Kvarnström, and T. Kunz, in L. Dunsch, B. Klatt, and W. Plieth (Eds.), Elektrochemie und Werkstoffe, GDCh Monographie, Frankfurt/M, 1995.
[26] J. Heinze, R. Bilger, unpublished results.
[27] M. Skompska, J. Mieczkowski, R. Holze, J. Heinze, J. Electroanal. Chem. 577 (2005) 9.
[28] D. Wei, T. Lindfors, C. Kvarnström, L. Kronberg, R. Sjöholm, A. Ivaska, J. Electroanal. Chem. 575 (2005) 19.
[29] F. Cataldo, P. Maltese, European Polym. J. 38 (2002) 1791.
[30] J.-W. Chevalier, J.-Y. Bergeron, L.H. Dao, Macromolecules 25 (1992) 3325.
[31] J. Kan, R. Lv, S. Zhang, Synth. Met. 145 (2004) 37.
[32] D. Orata, D.A. Buttry, J. Am. Chem. Soc. 109 (1987) 3574.
[33] H. Neugebauer, A. Neckel, N.S. Sariciftci, H. Kuzmany, Synth. Met. 29 (1989) 185.
[34] A. Moser, H. Neugebauer, K. Maurer, J. Theiner, A. Neckel, Springer Series Solid State Sci. 107 (1992) 276.
[35] I. Harada, Y. Furukawa, F. Ueda, Synth. Met. 29 (1989) 303.
[36] K.C. Persaud, Mater. Today 8 (2005) 38.